Hwang, K. J. (1984) in *Liposome Technology*, (Gregoriadis, G., Ed.) Vol. 3, pp 247-262, CRC, Boca Raton, FL.
Hwang, K. J., & Mauk, M. R. (1977) *Proc. Natl. Acad. Sci. U.S.A. 74*, 4991-4995.
Kaslow, D. C. (1986) *Nucleic Acids Res. 14*, 6767.
Labedan, B., & Letellier, L. (1984) *J. Bioenerg. Biomembr. 16*, 1-9.
Lakowicz, J. R. (1983) *Principles of Fluorescence Spectroscopy*, pp 44-47, Plenum, New York.
Latchman, D. S., & Brickell, P. M. (1986) *Nucleic Acids Res. 14*, 9220.
Le Pecq, J.-B., & Paoletti, C. (1966) *Anal. Biochem. 17*, 100-107.
Mackay, D. J., & Bode, V. C. (1976a) *Virology 72*, 167-181.
Mackay, D. J., & Bode, V. C. (1976b) *Virology 72*, 154-166.
Maniatis, T., Fritsch, E. F., & Sambrook, J. (1982) *Molecular Cloning: A Laboratory Manual*, pp 76-84, Cold Spring Harbor Laboratory, Cold Spring Harbor, NY.
Mimms, L. T., Zampighi, G., Nozaki, Y., Tanford, C., & Reynolds, J. (1981) *Biochemistry 20*, 833-840.
Peterson, G. L. (1977) *Anal. Biochem. 83*, 346-356.
Philippot, J., Mutaftschiev, S., & Liautard, J. P. (1983) *Biochim. Biophys. Acta 734*, 137-143.
Randall-Hazelbauer, L., & Schwartz, M. (1973) *J. Bacteriol. 116*, 1436-1446.
Roa, M. (1981) *FEMS Microbiol. Lett. 11*, 257-262.
Roa, M., & Scandella, D. (1976) *Virology 72*, 182-194.
Roessner, C. A., & Ihler, G. M. (1986) *J. Biol. Chem. 261*, 386-390.
Roessner, C. A., Struck, D. K., & Ihler, G. M. (1983) *J. Biol. Chem. 258*, 643-648.
Roessner, C. A., Struck, D. K., & Ihler, G. M. (1984) *Bio-Techniques 2*, 140-146.
Schwartz, M. (1975) *J. Mol. Biol. 99*, 185-201.
Schwartz, M. (1983) *Methods Enzymol. 97*, 100-112.
Schwartz, M., & Le Minor, L. (1975) *J. Virol. 15*, 679-685.
Szmelcman, S., & Hofnung, M. (1975) *J. Bacteriol. 124*, 112-118.
Weinstein, J. N., Ralston, E., Leserman, L. D., Klausner, R. D., Dragsten, P., Henkart, P., & Blumenthal, R. (1984) in *Liposome Technology* (Gregoriadis, G., Ed.) Vol. 3, pp 183-204, CRC, Boca Raton, FL.
Zarybnicky, V., Zarybnicka, A., & Frank, H. (1973) *Virology 54*, 318-329.
Zgaga, V., Medic, M., Salaj-Smik, E., & Novak, D. (1973) *J. Mol. Biol. 79*, 697-708.

Interparticle Interactions and Structural Changes of Nucleosome Core Particles in Low-Salt Solution†

Mitsuhiro Hirai,*,‡ Nobuo Niimura,§ Mitsuo Zama,∥ Kazuei Mita,∥ Sachiko Ichimura,∥ Fumio Tokunaga,⊥ and Yoshikazu Ishikawa⊥

Kanagawa Institute of Technology, Atsugi 243-02, Japan, Laboratory of Nuclear Science, Tohoku University, Sendai 982, Japan, Division of Chemistry, National Institute of Radiological Sciences, Chiba 260, Japan, and Physics Department, Tohoku University, Sendai 980, Japan

Received January 4, 1988; Revised Manuscript Received June 8, 1988

ABSTRACT: The structural behavior of the nucleosome core particles in the range of solvent Na^+ concentration from 10.45 to 0.45 mM has been studied by small-angle neutron and synchrotron radiation X-ray scattering, sedimentation, atomic absorption spectroscopy, density measurements, and circular dichroism. With decreasing salt concentration, the appearance of a scattering peak that is assignable to interparticle interactions, an intraparticle structural transition, a decrease in the sedimentation velocity of the particle, and a release of bound Na^+ ions from the particle are all observed concurrently when the ratio of solvent Na^+ ions per particle is below ~1000. These observations are interpreted to indicate that a release of bound Na^+ ions from the particle brings about structural rearrangements and weakens the electrostatic shielding of the particle, and this introduces long-range repulsive ordering of the particle in low-salt solution. Analyses of the scattering data indicate that the rearrangement within the core particle in low-salt solution is slight, changing the particle's shape slightly from cylindrical to a more spherical form by moving the center of the mass of the DNA somewhat inward with accompanying small decreases in the radii of gyration of both the DNA and the histones.

The basic structural features of the nucleosome have been established. The recent results of X-ray diffraction studies of crystals of nucleosome core particles (Richmond et al., 1984; Überbacher & Bunick, 1985) and histone–DNA cross-linking studies (Bavykin et al., 1985) afford a detailed knowledge of the three-dimensional structure of the core particle. However, the dynamical structural properties of nucleosomes in solution are indeterminate and are a subject of current interest because of their possible relation to different conformations that nucleosome might adopt during transcription and replication.

Many investigators have addressed this problem by examining the response of nucleosome core particles as polyelectrolytes in solution to reduction of ionic strength. The methods that have been applied include hydrodynamics (Gordon et al., 1978, 1979; Burch & Martinson, 1980; Libertini & Small, 1980; Harrington, 1981), fluorescence (Zama et al., 1978;

† This work was supported by a grant-in-aid from the Ministry of Education and by special coordination funds from the Science and Technology Agency of the Japanese government.
* Author to whom correspondence should be addressed.
‡ Kanagawa Institute of Technology.
§ Laboratory of Nuclear Science, Tohoku University.
∥ National Institute of Radiological Sciences.
⊥ Physics Department, Tohoku University.

0006-2960/88/0427-7924$01.50/0

Dieterich et al., 1979; Eshaghpour et al., 1980; Libertini & Small, 1982, 1987), electrooptical techniques (Crothers et al., 1978; Wu et al., 1979; Hantz et al., 1983), cross-linking (Martinson et al., 1979), and neutron scattering (Überbacher et al., 1983; Sibbet et al., 1983). Although the results of these studies support the view that a single unfolding transition occurs at about 1 mM monovalent salt concentration, the mechanism of the transition and details of the unfolded structure are still unsolved.

A nucleosome core particle contains 292 negatively charged phosphate groups and only a net positive charge of ~150 of the core histone octamer. Decreasing the ionic strength of the solution reduces the ability of the solvent to screen the Coulombic interactions between the charged groups on nucleosome and causes the net electrostatic free energy of the particle to increase. This may induce structural transition if there is another structure whose electrostatic free energy is lower. Another possibility, to which little attention has been paid, is that an interaction between nucleosome core particles may be changed or induced by decreasing the concentration of screening counterions.

In the present study, we have used several different physicochemical approaches including small-angle neutron and synchrotron radiation X-ray scatterings, sedimentation, atomic absorption spectroscopy, density measurements, and circular dichroism to solve this complex mechanism of the transition. These measurements were done as a function of the solvent Na^+ ion concentration ranging from 10.45 to 0.45 mM and the particle concentration ranging from 10.4 to 0.06 mg/mL. By combining all the data obtained by these different methods, we have consistently shown that interparticle interaction and conformational changes occur simultaneously at reduced ionic strength due to a drastic decrease in the number of bound counterions per particle. The results of the present work suggest that the interpretations or the analyses of some previous results on the nucleosome structure at low ionic strength have to be reconsidered.

Materials and Methods

Preparation of Nucleosome Core Particles. Nucleosome core particles were prepared from chicken erythrocytes by a method described elsewhere (Ichimura et al., 1982). H1- and H5-depleted chromatin was digested with micrococcal nuclease, and the monomer nucleosome fractions of 5–20% linear sucrose density gradient ultracentrifugation of the chromatin digests were collected to isolate core particles. The core particles thus obtained were further purified by the preparative polyacrylamide–agarose gel electrophoresis. For experiments at low ionic strength, a core particle solution (A_{260} = 1) was exhaustively dialyzed against 0.1 mM EDTA, pH 7.2, at 4 °C. Fresh deionized and distilled water was used throughout the experiment to prevent an accompanying risk of lowering the pH value due to absorption of carbon dioxide. The pH value of 6.8 was attained for the nucleosome solution after dialysis against 0.1 mM EDTA, pH 7.2. The concentration of Na^+ ions in the solvent 0.1 mM EDTA, pH 7.2, was determined to be 0.45 mM by atomic absorption spectroscopy. To prepare sample solutions of higher ionic strengths up to 10.45 mM used in the present study, varying amounts of concentrated NaCl solution in 0.1 mM EDTA (pH 7.2) were added to the nucleosome core solutions, which had been extensively dialyzed against 0.1 mM EDTA, pH 7.2, unless otherwise indicated.

Neutron Scattering. Small-angle neutron scattering experiments were carried out with the time-of-flight small-angle scattering spectrometer SAN installed at the pulsed neutron source KENS at the National Laboratory for High Energy Physics KEK, Tsukuba, Japan. The details of the design of this spectrometer and its parameters have been described (Ishikawa et al., 1986). The SAN is equipped with a 2D position-sensitive detector (60 × 60 cm) that consists of an array of 43 1D position-sensitive ^3He detectors. The range of wavelengths used was from 3 to 9 Å. The resolution of momentum transfer $\Delta Q/Q$ ($Q = 4\pi \sin\theta/\lambda$, where 2θ is the scattering angle and λ is wavelength) is about 30%. The sample–detector distance was 300 cm. The sample and buffer solutions were put in quartz cells of 20 mm in width and 40 mm in height with 2- or 5-mm path lengths. Sample exposures to neutron beam were in the range 1–6 h.

X-ray Scattering. Small-angle X-ray scattering experiments were carried out with small-angle scattering equipment SAXES installed at 2.5-GeV storage ring at the Photon Factory of KEK. The details of the optics and its performance can be referred to elsewhere (Ueki et al., 1985). The SAXES, by the use of focusing optics, has a small-angle resolution of Bragg spacing of 1000 Å. The wavelength used was 1.54 Å and the sample–detector distance was 190 or 80 cm. The sample cell of 1-mm path length has two thin quartz windows 5 mm in width and 3 mm in height. Quartz plates 50 μm thick were used for the windows. A 1D position-sensitive proportional counter, whose probe has 20 cm in effective length, is used for recording scattering intensities. The time of exposure of samples to the X-ray beam was 600 s, and the electron current in the storage ring was 70–150 mA.

Sedimentation Measurements. Sedimentation coefficients obtained with a Hitachi 282S analytical ultracentrifuge equipped with a UV scanner at 48 000 rpm were corrected to 20 °C. Migrating boundaries were recorded at 265 nm except for the studies on concentration dependence when A_{265} was higher than 1.0. In these cases boundaries were recorded at suitable optical densities in the wavelength range from 270 to 290 nm. Concentrations of the samples were determined by measuring the A_{260} with a Cary 17D spectrophotometer.

Atomic Absorption Spectroscopies. The number of bound counterions, Na^+, per nucleosome core particle was experimentally determined by using a Hitachi Model 170-70 Zeeman effect atomic absorption spectrophotometer. The experimental result was analyzed by the following formula. The total Na^+ concentration in the nucleosome core particle solution, C_t, can be expressed as

$$C_t = nC_1 + C_2 \quad (1)$$

where n is the number of bound Na^+ ions per nucleosome core particle and C_1 and C_2 are the concentration of nucleosome core particles in the solution and the free Na^+ ion concentration in the solution, respectively. C_t was determined by measuring the Na^+ concentration of the sample solution with the atomic absorption spectrophotometer. C_2 is approximately equal to the Na^+ concentration of the filtrate of the solution, C_2'. C_2' was determined by measuring the Na^+ concentration by atomic absorption measurements of the filtrate that had been obtained by vacuum (~50 mmHg) suction of the sample solution in a Collodion bag (Sartorius Membrane Filter Co. Ltd., pore size 8 nm) through the nitrocellulose membrane of the bag. If the excluded volume effect of the nucleosome core particles is taken into account, C_2 should be corrected as

$$C_2 = C_2' (1 - vMC_1) \quad (2)$$

where v is the excluded volume of the nucleosome core particle and M is its molecular weight. As the term vMC_1 is about 1.3×10^{-3} for the maximum C_1 used in the present study, 10^{-5} M, this term is negligible. Absorption wavelengths of 589.6

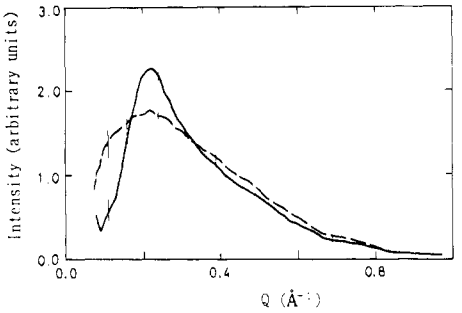

FIGURE 1: Comparison of the small-angle neutron scattering curves of the nucleosome core particle at high [10.45 mM (---)] and low [0.45 mM (—)] Na^+ concentrations. Samples at 10.45 mM Na^+ are dissolved in 94% D_2O/0.1 mM EDTA (pH 6.8)/10 mM NaCl, and those at 0.45 mM Na^+ are dissolved in 94% D_2O/0.1 mM EDTA (pH 6.8). Error bars are indicated by vertical lines.

and 330 nm of a hollow cathode lamp filled with Na gas were used for quantification of Na^+ ions. The sample volume used for one measurement was 10 μL; five independent measurements were done for the same sample, and the averaged values were taken. Prior to the measurements of Na^+ concentration of samples, a calibration curve was obtained by using standard solutions containing defined Na^+ concentrations.

Density Measurements. Apparent partial specific volumes of nucleosome core particles containing different salt concentrations were determined by measuring the densities of the sample solutions with an Anton Parr DMA 60 digital density meter by using a DMA 601 density measuring cell at 20 °C. Since the precision of the observed values is sensitive to temperature, the temperature fluctuation of the cell was minimized by a pair of temperature-controlled water circulators. Apparent specific volume, v_a, is given by

$$v_a = [1 - (\rho - \rho_0)/m]/\rho$$

where ρ, ρ_0, and m are the densities of the solution, the solvent, and the solute, respectively.

Circular Dichroism. Circular dichroism measurements were carried out on a Jasco J-20 spectropolarimeter at room temperature with a 2 mm path length cell. The same sample solutions as those used for the synchrotron X-ray scattering experiments (A_{260} = 5) were used for the circular dichroism measurements. The molar extinction coefficient of DNA at 260 nm (ϵ_p = 6500) was used in calculations of the molar ellipticity expressed as moles of nucleotides, $[\Theta]_p$.

RESULTS

Neutron and X-ray Scattering Measurements. Small-angle neutron scattering measurements were done for nucleosome core samples in D_2O at different solvent sodium ion concentrations ranging from 0.45 to 10.45 mM. The neutron scattering curves at a particle concentration of 10.4 mg/mL are shown in Figure 1. It is found that at a low Na^+ concentration of 0.45 mM a single peak is clearly observed, whereas this peak gradually decays with broadening of its width with increasing solvent Na^+ concentration; at the highest salt concentration examined (10.45 mM) the peak becomes almost undetectable. This tendency does not depend on the solute concentration in the range 10.4–5.6 mg/mL used in our neutron scattering measurements. The results of a series of small-angle X-ray scattering measurements using synchrotron radiation that have been done with the nucleosome core samples of lower concentration (5.85–0.5 mg/mL) also demonstrated similar tendencies. The positions of the peak observed from both neutron and X-ray scattering studies of samples of different concentrations at a low ionic strength (0.45 mM) are listed in Table I. From the table, and as is also shown in Figure 2, it is apparent that the peak position shifts toward the smaller Q region with lower sample concentration. These observations strongly suggest that the peak in the scattering curve is originated from interparticle interactions that are induced at reduced ionic strength. The peaks are located at the Q values we expect from corresponding solute concentrations. This further suggests that the core particles in low-salt solution are dispersed somewhat nonrandomly due to particle–particle interactions. The possibility of an aggregate formation in the present systems can be ruled out by the following observations. If aggregates are formed, the scattering curve continuously rises, without making a peak, down to low Q regions where a damping by a beam stopper occurs. Furthermore, neither decrease in sample concentrations nor increase in sedimentation velocity due to aggregation was detected in the present nucleosome core samples.

In order to examine changes in shape of the nucleosome core particle that might be induced at reduced ionic strength, scattering at the high Q regions was measured by the synchrotron radiation X-ray source, where the background scattering is very low. In Figure 3 are shown the log (INT) versus log Q plots of the nucleosome core particles (0.585

Table I: Scattering Peak Positions of Nucleosome Core Particle Solutions at Different Sample Concentrations[a]

nucleosome concn (mg/mL)	peak position ($Å^{-1}$)	nucleosome concn (mg/mL)	peak position ($Å^{-1}$)
10.4	0.022	2.0	0.012
8.5	0.020	1.0	0.010
5.6	0.018	0.5	0.009
5.85	0.017		

[a] The peak positions for the samples of 10.4, 8.5, and 5.6 mg/mL were determined by neutron scattering, and those for the samples of 5.85, 2.0, 1.0, and 0.5 mg/mL were determined by X-ray scattering using synchrotron radiation. All samples were dissolved in 0.1 mM EDTA, pH 6.8.

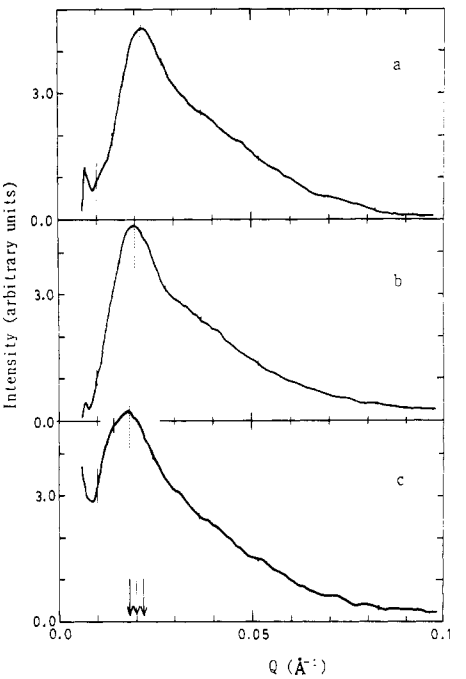

FIGURE 2: Small-angle neutron scattering curves of nucleosome core particles at different sample concentrations at a low (0.45 mM) Na^+ concentration. Sample concentrations are (a) 10.4, (b) 8.5, and (c) 5.6 mg/mL. Samples are dissolved in 94% D_2O/0.1 mM EDTA (pH 6.8). Dotted lines and arrows indicate the positions of the peaks of the scattering curves. Error bars are indicated by vertical lines.

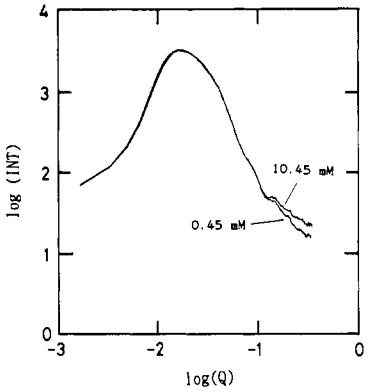

FIGURE 3: Comparison of the synchrotron radiation small-angle X-ray scattering curves at high Q regions of the nucleosome core particle solutions at high (10.45 mM) and low (0.45 mM) solvent Na^+ concentration ionic strengths. Sample concentration is 5.85 mg/mL.

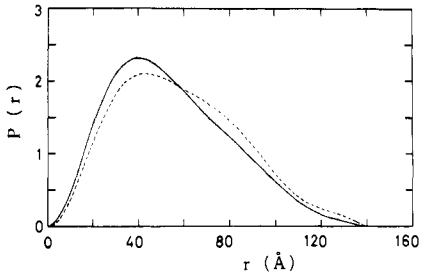

FIGURE 4: Comparison of the length distribution functions of the nucleosome core particle at high [10.45 mM (---)] and low [0.45 mM (—)] Na^+ concentrations. Samples at 10.45 mM Na^+ are dissolved in 0.1 mM EDTA (pH 6.8)/10 mM NaCl, and those at 0.45 mM Na^+ are dissolved in 0.1 mM EDTA (pH 6.8). Synchrotron radiation small-angle X-ray scattering data obtained at 2.0 mg/mL sample concentration were used.

mg/mL) at 10.45 and 0.45 mM Na^+ obtained by X-ray scattering measurements. From a comparison of the two scattering curves it is obvious that the intensity of the curve at 10.45 mM salt is greater than that at 0.45 mM salt above 0.09 $Å^{-1}$. Similar changes in the scattering curves at low ionic strength were seen irrespective of particle concentrations examined down to 0.50 mg/mL. The observed change in the scattering curve indicates that the shape of the core particle changes slightly from cylindrical to spherical form as the solvent ionic strength decreases from 10.45 to 0.45 mM.

The length distribution functions obtained by Fourier inversion of the scattering data at 10.45 and 0.45 mM Na^+ concentrations are shown in Figure 4. This function represents the distribution of the intramolecular distances (r). It can be seen that in comparison with the length distribution of the core particle at high salt the center of the length distribution of the particle at low salt is shifted to smaller distances, suggesting that the material with higher scattering length density moves toward the center of the nucleosome core particle at low ionic strength. The zero cross point at longer distance corresponds to the longest length of the intramolecular vector. The results that either of the two length distribution functions has the zero cross point at 140 Å indicate that there is no major change in the particle diameter with ionic strength.

We next carried out Guinier analysis of the scattering data. Because of the existence of the scattering peak of interparticle interactions, it is difficult to obtain an accurate radius of gyration, R_g, of the core particle from the Guinier plot, especially at low salt concentration. We therefore used the outside of the peak ($Q > 0.025$ $Å^{-1}$), where the scattering profile is almost independent of interparticle interactions, to obtain the radius of gyration and tentatively chose the Q range

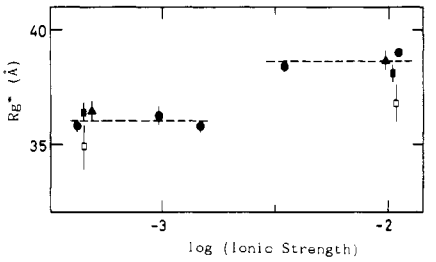

FIGURE 5: Apparent radius of gyration, R_g^*, of the nucleosome core particle as a function of ionic strength: (▲) 5.6 mg/mL in D_2O; (●) 8.5 mg/mL in D_2O; (■) 10.4 mg/mL in D_2O; (□) 7.8 mg/mL in 65% D_2O. To calculate R_g^* values the Q range 0.025–0.05$Å^{-1}$ was used.

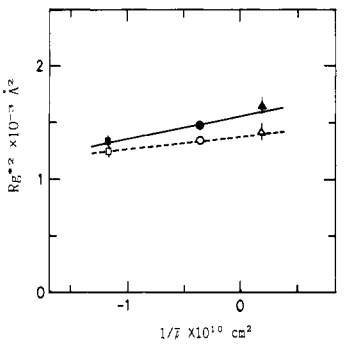

FIGURE 6: Variation of R_g^{*2} of the nucleosome core particle as a function of $1/\bar{\rho}$: (---) 0.45 mM Na^+; (—) 10.45 mM Na^+. The data points ▲ and △ were obtained by synchrotron radiation small-angle X-ray scattering measurements, and the other points, ●, ○, ■, and □, were obtained by small-angle neutron scattering measurements.

0.025–0.05 $Å^{-1}$ to calculate an apparent radius of gyration denoted by R_g^*. A similar Q region has been used by other authors to calculate R_g values of the nucleosome core particles (Pardon et al., 1975; Sibbet et al., 1983).

The R_g^* values thus calculated are plotted as a function of ionic strength in Figure 5. The R_g^* value at 10.45 mM Na^+ in 100% D_2O, 38.6 Å, is close to those obtained by other authors (Pardon et al., 1975; Überbacher et al., 1983) under comparable solvent conditions. At a reduced solvent Na^+ concentration of 0.45 mM, the R_g^* decreases to 36.2 Å. With decreasing ionic strength, a transition in the R_g^* value occurs at 3–~1.5 mM solvent Na^+ concentrations. The apparent radius of gyration, R_g^*, obtained in H_2O from X-ray scattering of samples at lower particle concentrations showed similar changes with ionic strength (data not shown). In this case the R_g^* at 10.45 mM Na^+ ionic strength, 40.0 Å, decreased to 38 Å at 0.45 mM Na^+. The R_g^* values of the histones that were obtained in 65% D_2O, where the solvent scattering matches that of the DNA and so only the histones are seen, also decrease from 36.8 Å at 10.45 mM Na^+, to 34.9 Å at 0.45 mM Na^+, as shown in Figure 5.

Stuhrmann (1974) has demonstrated that, for an inhomogeneous but essentially centrosymmetric particle, R_g will vary as $R_g^2 = R_0^2 + \alpha/\bar{\rho}$, where R_0 is the radius of gyration of the particle at infinite contrast ($\bar{\rho} = \infty$) and $\bar{\rho}$ the difference between the mean scattering length density of the particle and the solvent. α has the significance of a mean square distance of fluctuations of scattering length density from the center of shape. The plots of R_g^{*2} versus $1/\bar{\rho}$ (Stuhrmann plots) for the nucleosome core particles in 10.45 and 0.45 mM Na^+ are shown in Figure 6. The positive slopes for the plots indicate that the material with higher scattering density in the nucleosome core particle (the DNA) is located outside the material with lower scattering density (the histones) in either ionic strength. However, the measured value of the slope, α, for

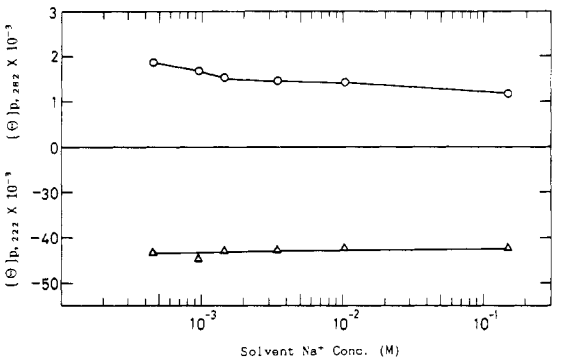

FIGURE 7: Changes of molar ellipticities at 282 nm ($[\Theta]_{P,282}$) and 222 nm ($[\Theta]_{p,222}$) of nucleosome cores as a function of solvent Na^+ concentration.

the core particle in 0.45 mM Na^+, $(150 \pm 80) \times 10^{-5}$, is smaller than that for the particle in 10.45 mM ionic strength, $(190 \pm 60) \times 10^{-5}$. This indicates that the mass of DNA of the core particle is shifted slightly inward in low-salt solvent in comparison with that in high-salt solvent and is consistent with the above-mentioned result of the analyses of the scattering data by length distribution function. At the y intercept ($\bar{p} = \infty$) of the R_g^{*2} versus $1/\bar{p}$ plot, the contrast between the particles and surrounding medium is infinite. In this situation, internal variations in scattering density are not significant, and R_g^* represents the apparent radius of gyration of the shape or surface of an essentially homogeneous particle. The apparent radii of gyration at infinite contrast, R_0^*, are 39.2 and 37.3 Å for the nucleosome core particle at 10.45 and 0.45 mM salt concentrations, respectively.

Circular Dichroism Measurements. Molar ellipticities at 282 nm ($[\Theta]_{282}$) and 222 nm ($[\Theta]_{222}$) of the core particle are plotted as a function of salt concentration in Figure 7. A slight increase in the value of $[\Theta]_{282}$ at reduced ionic strength seen in the plot is in agreement with the results of previous authors (Watanabe & Iso, 1981; Gordon et al., 1979; Libertini & Small, 1987) and indicates some minor structural change of the nucleosome core DNA. The value of $[\Theta]_{222}$ remains unchanged with salt concentration, indicating that no loss of the secondary structure of the histones occurs over the range of ionic strength examined. These results of circular dichroism are in general agreement with those of the scattering experiments described above.

Sedimentation Velocity Measurements. The measured sedimentation coefficients of the nucleosome core particles are shown in Figure 8 as a function of the logarithm of solvent Na^+ concentration ranging from 0.45 to 10.45 mM. The nucleosome core samples of different concentration over the range 0.062–1.9 mg/mL were used for the sedimentation measurements. The decrease in the sedimentation coefficients with decreasing ionic strength observed with samples at low nucleosome core concentrations (0.062–0.13 mg/mL) is similar to that reported by other authors (Gordon et al., 1978, 1979; Burch & Martinson, 1980; Libertini & Small, 1980; Überbacher et al., 1984). This decrease in $s_{20,w}$ has been attributed to conformational changes of the nucleosome core particle at low ionic strength. The sedimentation coefficients of the core particles at higher concentrations (0.4–1.9 mg/mL), which have not been reported to date in such a low ionic strength range, exhibit a marked particle concentration effect. The samples at higher concentration show more prominent decreases in sedimentation coefficients with decreasing solvent sodium ion concentration. The observed decrease in the sedimentation coefficient with increasing sample concentration excludes the possibility of an aggregate formation since this

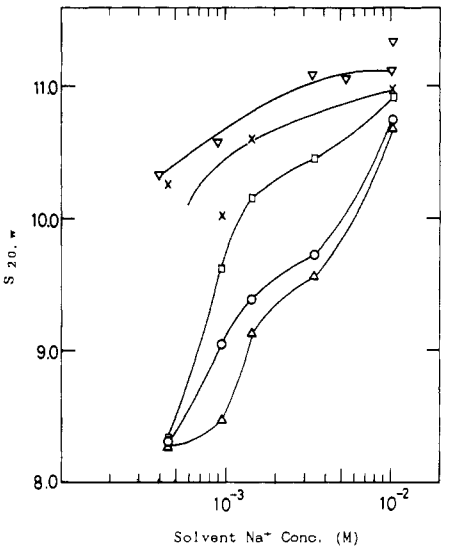

FIGURE 8: $s_{20,w}$ of the nucleosome core particle as a function of solvent Na^+ concentration. Sample Concentrations are (▽) 0.062–0.082, (×) 0.13, (□) 0.4, (○) 0.75 (△) 1.9 mg/mL. The solvent contained 0.1 mM EDTA except for the samples of 0.062–0.082 mg/mL, where 0.2 mM EDTA was used as the solvent.

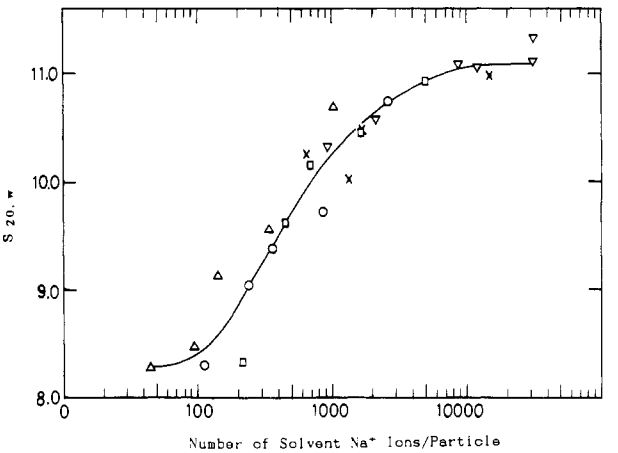

FIGURE 9: $s_{20,w}$ of the nucleosome core particle as a function of the number of solvent Na^+ ions per particle. The data points in Figure 8 were replotted. The symbols used correspond to those in Figure 8.

usually increases in the sedimentation velocity.

In Figure 9 the measured $s_{20,w}$ values are plotted as a function of the number of solvent Na^+ ions per nucleosome core particle. Interestingly, in contrast to the plots in Figure 8 in which $s_{20,w}$ varied widely depending on nucleosome core concentration, changes in $s_{20,w}$ are represented by a single sigmoidal curve in this plot with a midpoint of the transition of the $s_{20,w}$ value at 500–600 solvent Na^+ ions/particle. Above 10000 Na^+ ions/particle the $s_{20,w}$ reaches a plateau value. This plot suggests that the sedimentation velocity of the nucleosome core particle is determined by the number of solvent counterions per particle rather than solvent ionic strength or particle concentration per se.

Atomic Absorption Spectroscopy and Density Measurements. As a next step, flameless atomic absorption spectroscopy studies were done on aliquots from the same sample solutions used for sedimentation measurements to determine the number of bound Na^+ ions per nucleosome core particle. It was found that, as shown in Figure 10, with decreasing number of solvent Na^+ ions per particle below 1000 the number of bound Na^+ ions per particle decreases from 400–350 to 300–150. The midpoint of the transition of the

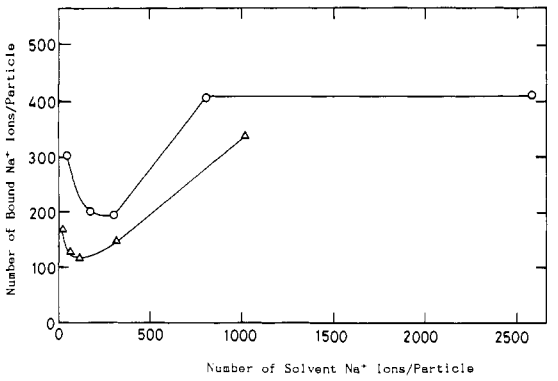

FIGURE 10: Changes in the number of bound Na^+ ion per particle as a function of the number of solvent Na^+ ions per particle. Sample concentrations are (○) 0.75 and (△) 1.9 mg/mL. The number of bound Na^+ ions per particle was determined by atomic absorption spectroscopy.

number of bound counterions, which is positioned at 600–500 solvent Na^+ ions/particle, coincides with the midpoint for the $s_{20,w}$ value transition. The results suggest that this dramatic release of some 100 Na^+ ions/particle is correlated with the reduction in the sedimentation velocity of the nucleosome core particle at low ionic strength.

The apparent partial specific volume of the nucleosome core particle was also determined by measuring the densities of the sample solutions with a digital density meter. The average values of the apparent specific volumes with samples at 1.90 and 1.10 mg/mL were 0.663 and 0.625 mL/g at 10.45 and 0.45 mM Na^+, respectively. The value at 10.45 mM Na^+ is close to the apparent volume of 0.65 mL/g in 0.1–0.5 M NaCl (Ausio et al., 1984) and an earlier value of 0.661 mL/g in 10 mM KCl (Olins et al., 1976).

Discussion

The results of the present neutron and X-ray scattering studies indicate that, by reducing the ionic strength of the nucleosome core particle solution from 10.45 to 0.45 mM, interparticle interactions and small intraparticle structural changes are induced simultaneously. The sedimentation and atomic absorption spectroscopy studies have shown that the decrease in the $s_{20,w}$ value of the core particle at low ionic strength parallels the decrease in the number of solvent Na^+ ions per particle and is correlated with a dramatic release of bound Na^+ ions.

The evidence for the existence of interparticle interactions in low-salt solutions was provided by the appearance of a new peak in the scattering curve, most prominently at the lowest solvent Na^+ concentration examined, 0.45 mM. The existence of this peak has not been reported by previous neutron scattering studies on the nucleosome core particle by Überbacher et al. (1983) and Sibbet et al. (1983), despite the comparable sample concentration and solvent ionic strengths employed. This might be due to the fact that we could collect the scattering data at low Q values with a camera at the KEK synchrotron radiation X-ray source, where the background scattering is very low. The higher particle concentration employed in the present neutron scattering study also helped us to detect the peak easily, because it makes the peak shift toward high Q regions with higher scattering intensity.

Changes in the scattering curve at high Q region have indicated that the nucleosome core particle slightly changes its shape from cylindrical to spherical in low-salt solvents. The analyses of the scattering data by the Stuhrmann plots and the length distribution function have further shown that the core DNA moves somewhat toward the center of the core particle at reduced ionic strength, without changing the particle diameter. The radius of gyration R_g* of the core particle decreases by 2.4 Å at 1.5–3 mM Na^+ concentration with decreasing solvent Na^+ concentration from 10.45 to 0.45 mM. Überbacher et al. (1983) have shown by neutron scattering that the R_g of the nucleosome core particle increases, but not decreases, by 10 Å at low ionic strength ($<\sim 2$ mM). This discrepancy might be due to the fact that in the analysis of the scattering data we took into consideration the scattering peak of interparticle interactions. Neutron scattering studies by Sibbet et al. (1983), on the other hand, have detected no change in the radii of gyration of the core particles down to an ionic strength of 2.0 mM. The ionic strength they used may not be low enough to induce structural changes. The R_g* values of the histone octamer that were calculated from the Guinier plots of the neutron scattering curve at 65% D_2O showed only a slight decrease (1.9 Å) at low solvent Na^+ concentration.

There are a number of studies which indicate that changes in histone conformation and histone–histone interactions take place at low ionic strength. Fluorescence studies have demonstrated that the labeled cysteine residues of H3 move somewhat apart and become accessible to solvent (Zama et al., 1978; Dieterich et al., 1979) and that the labeled methionine residues of H4 experience some environmental change in low-salt solvent (Chung & Lewis, 1985, 1986). The intrinsic tyrosine fluorescence of the core particle suggests disruption of histone–histone interaction or changes in the histone secondary structure (Libertini & Small, 1980, 1982). The results of the histone–histone UV cross-linking studies (Martinson et al., 1979) have also shown that the H2B–H4 contacts are ruptured at low ionic strength. Although it is difficult to reach a consensus as to the degree of structural changes of the core histones from these studies, it is most likely that the changes they detected reflect internal rearrangements of the histones, which have little effect on the gross shape of the histone octamer.

The change in $s_{20,w}$ values of the core particles with ionic strength exhibited a marked concentration dependency. Nucleosome core samples of higher concentrations have smaller $s_{20,w}$ values over the ionic strength range examined. We have shown that this concentration effect on the sedimentation velocity is interpreted in terms of the number of solvent Na^+ ions per particle, rather than the sample concentration or the solvent ionic strength per se. The $s_{20,w}$ decreases with decreasing number of solvent counterions per particle, and the transition midpoint is at 600–500 solvent Na^+ ions/particle. Atomic absorption spectroscopy studies have shown that around this midpoint a drastic reduction of the number of bound counterions from 400–350 to 300–150 occurs. Wu et al. (1979), by analyzing the unfolding transition curve of transient electric dichroism, have suggested that at least 2–3 ions/particle are released when the nucleosome core particle unfolds in low salt. The number of released counterions of some 100 Na^+ that we have experimentally determined is much larger than that they estimated.

In summarizing the results, we have shown here that during the course of the reduction of ionic strength of the nucleosome core particle solutions, interparticle interactions, intraparticle structural changes, reductions in $s_{20,w}$ values, and a release of counterions are all concurrently induced in the region below ~ 1000 of solvent Na^+ ions/particle. All these characteristic behaviors in low-salt solution of the nucleosome core particles might be interrelated in the following manner. The core particle has 146 net negative electronic charges. The release

of bound Na^+ ions from the particle brings about intraparticle structural rearrangements and weakens the electrostatic shielding of the particle, and this introduces long-range electrostatic repulsive ordering of the particle in low-salt solution, resulting in the appearance of the prominent scattering peaks of interparticle interactions and a marked reduction of $s_{20,w}$ values of nucleosome core particles. The observed small changes of the core particle in our preparation by decreasing the solvent Na^+ ion concentration to 0.45 mM do not necessarily contradict the measurements made by others with different preparations, who may have reached lower salt concentrations (Wu et al., 1979; Harrington et al., 1981; Libertini & Small, 1987; Libertini et al., 1988). Because of the large sedimentation velocity of the nucleosome core particle compared with that of Na^+, the ionized core particle sediments more rapidly than the counterions. The distribution of the charge results in a potential gradient against the direction of sedimentation, which tends to reduce the $s_{20,w}$ of the core particle, especially when sedimentation is carried out in a solution of low ionic strength. This charge effect (Eisenberg, 1976), in addition to changes of core particle shape and interparticle interactions, may also decrease the $s_{20,w}$ values of the nucleosome core particle in low-salt solution.

The present interpretation of the result of the sedimentation is in contrast to that attributing the decrease in the $s_{20,w}$ of the nucleosome core particle at low ionic strength solely to conformational changes or unfolding of the particle. The hydrodynamic behaviors of the nucleosome core particles at much higher salt concentrations, e.g., >0.01 M NaCl, where enough shielding counterions exist, are consistent with the present view. That is, as has been reported by Ausio et al. (1984), the values of $s_{20,w}$ in 0.6 M NaCl are independent of particle concentration and the values of the apparent volumes of the particle are independent of salt concentration over the range 0.1–0.5 M NaCl.

On the basis of the present observations it is of interest to consider the physical mechanism responsible for the structural changes of the nucleosome core particle at low ionic strength. The nucleosome core contains 1.75 superhelical turns of 146 base pair DNA. Therefore, two ~60 base pair segments of DNA lie adjacent to each other on the circumference of the disk, with the edges of the DNA double-helices separated by only 5–10 Å. Removal of the screening counterions increases the repulsion between these overlapping portions of DNA. At a solvent salt concentration of 500–600 Na^+/particle the disk of the core particle changes the structure to spherical shape by removing the overlap of DNA segments to the direction of the axis of the disk. The histone–DNA binding, on the other hand, is rather strengthened by decreasing the ionic strength of the solution. The constraints imposed on DNA by binding with the histones might inhibit the superhelix of the DNA to expand or unfold. In spite of the net negative charge density of the nucleosome core particle, it is possible that there are local regions of net charge density whose mutual repulsion contributes to reduction of the free energy of the structural changes in low salt. For example, removal of screening anions from the positively charged N- and C-terminal regions of the histones H2A and H2B, which remain mobile within the core particle (Cary et al., 1978), could increase electrostatic repulsion. Some local charge redistribution within the core particle induced as a result of the low-salt structural change may explain the dramatic release of bound Na^+ ions from the particle.

The electrostatic repulsion ordering of the nucleosome core particle in low-salt solutions is also interesting because of its possible biological implications. The distance between the interacting particles estimated from the observed scattering peak position coincides with the average particle–particle distance calculated from the particle concentration. The repulsive nucleosome–nucleosome interaction, which has been found in the present study to be induced at low salt concentration (<10 mM Na^+), may be one of the driving forces to disrupt the chromatin 30-nm fiber structure to 10-nm fiber structure, typically around 1 mM NaCl (Thoma et al., 1979). In chromatin in low-salt solvent, electrostatic repulsions between the linker DNA and the core DNA, which are brought close to each other within the 30-nm fiber, may also facilitate the formation of the extended 10-nm nucleofilament. Neutron scattering experiments that are designed to elucidate the physical bases of the folding of the chromatin filament to higher order structure are now in progress in our laboratory.

ACKNOWLEDGMENTS

We thank Prof. Kaji and Prof. Ueki for helpful criticisms and suggestions.

Registry No. Na, 7440-23-5.

REFERENCES

Ausio, J., Seger, D., & Eisenberg, H. (1984) *J. Mol. Biol. 176*, 77–104.

Bavykin, S. G., Usachenko, S., Lishanskaya, A. I., Zalenskaya, I. A., & Mirzabekov, A. D. (1985) *Nucleic Acids Res. 13*, 3439–3459.

Burch, J. B. E., & Martinson, H. G. (1980) *Nucleic Acids Res. 8*, 4969–4987.

Cary, P., Moss, T., & Bradbury, E. M. (1978) *Eur. J. Biochem. 89*, 475–482.

Chung, D. G., & Lewis, P. N. (1985) *Biochemistry 24*, 8028–8036.

Chung, D. G., & Lewis, P. N. (1986) *Biochemistry 25*, 2048–2054.

Crothers, D. M., Dattaguputa, N., Hogan, M., Klevan, L., & Lee, K. S. (1978) *Biochemistry 17*, 4525–4533.

Dieterich, A. E., Axel, R., & Cantor, C. R. (1979) *J. Mol. Biol. 129*, 587–602.

Eisenberg, H. (1976) *Biophys. Chem. 5*, 243–251.

Eshaghpour, H., Dieterich, A. E., Cantor, C. R., & Crothers, D. M. (1980) *Biochemistry 19*, 1797–1805.

Gordon, V. C., Knobler, C. M., Olins, D. E., & Schumaker, V. N. (1978) *Proc. Natl. Acad. Sci. U.S.A. 75*, 660–663.

Gordon, V. C., Schumaker, V. N., Olins, D. E., Knobler, C. M., & Horwitz, J. (1979) *Nucleic Acids Res. 6*, 3845–3858.

Hantz, E., Coa, A., Taillandier, E., Tivant, P., Drifford, M., Defer, N., & Kruh, J. (1983) *Int. J. Biol. Macromol. 5*, 130–134.

Harrington, R. E. (1981) *Biopolymers 20*, 719–752.

Ichimura, S., Mita, K., & Zama, M. (1982) *Biochemistry 21*, 5329–5334.

Ishikawa, Y., Furusaka, M., Niimura, N., Arai, M., & Hasegawa, K. (1986) *J. Appl. Crystallogr. 19*, 229–242.

Libertini, L. J., & Small, E. W. (1980) *Nucleic Acids Res. 8*, 3517–3534.

Libertini, L. J., & Small, E. W. (1982) *Biochemistry 21*, 3327–3334.

Libertini, L. J., & Small, E. W. (1987) *Nucleic Acids Res. 15*, 6655–6664.

Libertini, L. J., Ausio, J., van Holde, K. E., & Small, E. W. (1988) *Biophys. J. 53*, 477–487.

Martinson, H. G., True, R. J., & Burch, J. B. E. (1979) *Biochemistry 18*, 1082–1088.

Olins, A. L., Carlson, R. D., Wright, E. B., & Olins, D. E. (1976) *Nucleic Acids Res. 3*, 3271–3291.
Pardon, J. F., Worcester, D. L., Wooley, J. C., Tatchell, K., van Holde, K. E., & Richards, B. M. (1975) *Nucleic Acids Res. 2*, 2163–2176.
Richmond, T. J., Finch, J. T., Rushton, B., Rhodes, D., & Klug, A. (1984) *Nature (London) 311*, 532–537.
Sibbet, G. J., Carpenter, B. G., Ibel, K., May, R. P., Kneale, G. G., Bradbury, E. M., & Baldwin, J. P. (1983) *Eur. J. Biochem. 133*, 393–398.
Stuhrmann, H. B. (1974) *J. Appl. Crystallogr. 7*, 173–178.
Thoma, F., Koller, Th., & Klug, A. (1979) *J. Cell Biol. 83*, 403–427.
Überbacher, E. C., & Bunick, G. J. (1985) *J. Biomol. Struct. Dyn. 2*, 1033–1055.
Überbacher, E. C., Ramakrishnan, V., Olins, D. E., & Bunick, G. J. (1983) *Biochemistry 22*, 4916–4923.
Ueki, T., Hiragi, Y., Kataoka, M., Inoko, Y., Amemiya, Y., Izumi, Y., Tagawa, H., & Muroga, Y. (1985) *Biophys. Chem. 23*, 115–124.
Watanabe, K., & Iso, K. (1981) *J. Mol. Biol. 151*, 143–163.
Wu, H., Dattagupta, N., Hogan, M., & Crothers, D. M. (1979) *Biochemistry 18*, 3960–3965.
Zama, M., Bryan, P. N., Harrington, R. E., Olins, A. L., & Olins, D. E. (1978) *Cold Spring Harbor Symp. Quant. Biol. 42*, 31–41.

Purification and NMR Studies of [*methyl*-^{13}C]Methionine-Labeled Truncated Methionyl-tRNA Synthetase†

Paul R. Rosevear
Department of Biochemistry and Molecular Biology, University of Texas Medical School, Houston, Texas 77225
Received January 13, 1988; Revised Manuscript Received June 9, 1988

ABSTRACT: A procedure for the rapid purification of a truncated form of the *Escherichia coli* methionyl-tRNA synthetase has been developed. With this procedure, final yields of approximately 3 mg of truncated methionyl-tRNA synthetase per gram of cells, carrying the plasmid encoding the gene for the truncated synthetase [Barker, D. G., Ebel, J.-P., Jakes, R., & Bruton, C. J. (1982) *Eur. J. Biochem. 127*, 449], can be obtained. The catalytic properties of the purified truncated synthetase were found to be identical with those of the native dimeric and trypsin-modified methionyl-tRNA synthetases. A rapid procedure for obtaining milligram quantities of the enzyme is necessary before the efficient incorporation of stable isotopes into the synthetase becomes practical for physical studies. With this procedure, truncated methionyl-tRNA synthetase labeled with [*methyl*-^{13}C]methionine was purified from an *Escherichia coli* strain auxotrophic for methionine and containing the plasmid encoding the gene for the truncated methionyl-tRNA synthetase. Both carbon-13 and proton observe–heteronuclear detect NMR experiments were used to observe the ^{13}C-enriched methyl resonances of the 17 methionine residues in the truncated synthetase. In the absence of ligands, 13 of the 17 methionine residues could be resolved by carbon-13 NMR. Titration of the synthetase, monitoring the chemical shifts of resonances B and M (Figure 3), with a number of amino acid ligands and ATP yielded dissociation constants consistent with those derived from binding and kinetic data, indicating active site binding of the ligands under the conditions of the NMR experiment. The maximum chemical shift change of resonance B, in the presence of saturating concentrations of ligands, was found to be dependent on the exact nature of the amino acid side chain. Differences in the magnitude of the substrate-induced conformational change, detected by monitoring resonance B, may be critical in triggering the recognition processes between cognate amino acid and synthetase. In contrast, the chemical shift of resonance M was found to be dependent on the negative charge introduced by the ligands at the aminoacyl adenylate site. This correlation is consistent with an induced-fit mechanism where portions of the binding site are formed as the various ligands are introduced into the aminoacyl adenylate site. Further studies on the solution structure of synthetase–ligand complexes will be useful in probing the structural mechanisms used in catalysis and amino acid discrimination.

The methionyl-tRNA synthetase is a member of a family of enzymes responsible for ligation of specific amino acids to their cognate tRNAs (Schimmel & Soll, 1979). This reaction occurs in two separate steps, and the specificity exhibited toward the substrates in each step is essential in maintaining the fidelity of information transfer from DNA to protein. The *Escherichia coli* methionyl-tRNA synthetase is a dimeric zinc metalloprotein with an apparent subunit molecular mass of 76 000 daltons (Barker et al., 1982). Two ATP binding sites per subunit have been found for the native dimeric enzyme (Fayat & Waller, 1974). The role of the second ATP binding site is unknown. Mild proteolysis with trypsin is known to produce a fully active monomeric fragment with an apparent molecular mass of 64 000 daltons (Cassio & Waller, 1974). The active trypsin fragment is produced by removal of about 130 amino acid residues from the carboxy terminus of the native protein. Kinetic properties of the trypsin fragment were found to be identical with those of the native dimeric enzyme (Blanquet et al., 1974; Hayafil et al., 1976). However, the monomeric enzyme was found to have only a single ATP binding site, it being the catalytic site (Fayat & Waller, 1974).

† This work was supported by a grant from the Robert A. Welch Foundation, AU-1025.

0006-2960/88/0427-7931$01.50/0